analytical chemistry

March 15, 2001

MICHAEL BROWN—UNIVERSITY OF SOUTH CAROLINA

http://pubs.acs.org/ac

Accelerated Articles
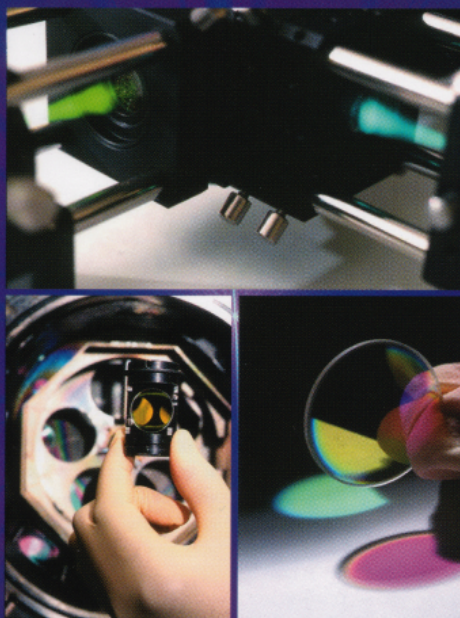
Design and Testing of a Multivariate Optical Element: The First Demonstration of Multivariate Optical Computing for Predictive Spectroscopy

O. Soyemi,[†] D. Eastwood,[†] L. Zhang,[†] H. Li,[†] J. Karunamuni,[†] P. Gemperline,[‡] R. A. Synowicki,[§] and M. L. Myrick*,[†]

Department of Chemistry and Biochemistry, University of South Carolina, Columbia, South Carolina 29208, Department of Chemistry and Biochemistry, East Carolina University, Greenville, North Carolina 27258, and J. A. Woollam Company Inc., 645 M Street, Suite 102, Lincoln, Nebraska 68508

A demonstration of multivariate optical computing is presented using binary dye mixtures consisting of Bismarck Brown and Crystal Violet. Bismarck Brown was treated as the analyte, while Crystal Violet was treated as a random interfering species. First, a multilayer multivariate optical element (MOE) for the determination of Bismarck Brown was designed using a novel nonlinear optimization algorithm. Next, the MOE was fabricated by depositing alternating layers of two metal oxide films (Nb_2O_5 and SiO_2) on a BK-7 glass substrate via reactive magnetron sputtering. Finally, the MOE was tested on 39 binary dye mixtures using a simple T-format prototype instrument constructed for this purpose. For each sample, measurements of the difference between transmittance through the MOE, and the reflectance from the MOE were made. By setting aside some of the samples for instrument calibration and then using the calibration model to predict the remaining samples, a standard error of prediction of 0.69 μM was obtained for Bismarck Brown using a linear regression model.

Multivariate calibration is an established tool in chemometrics for the correlation of a physical or chemical property of interest to information spanning multiple wavelength channels in optical spectroscopy.[1−3] The conventional application of this tool in chemical analysis entails first the acquisition of optical spectra in the appropriate wavelength region (typically from the ultraviolet to the mid-infrared). Next, chemometric tools are used to extract a spectral pattern (the regression vector) which is correlated to the property of interest but orthogonal to interferences.[4] Prediction of the property in an unknown sample is then carried out by determining the magnitude of the spectral pattern in the optical spectrum of the sample. More specifically, the magnitude is calculated by taking the inner product of the regression vector and the optical spectrum of the unknown sample. A major drawback in the widespread use of multivariate calibration, especially for field applications, is its dependence on expensive and bulky laboratory-type equipment for data acquisition and analysis.

A recent publication from our laboratory[5] addressed from a theoretical standpoint the feasibility of using optical computing in predictive spectroscopy to simplify and harden the apparatus necessary for chemical prediction. The first reports of a related hypothetical optical approach to multivariate chemical measurement were those of Bialkowski.[6] The use of a single multivariate optical element (MOE) in a beam splitter configuration has also

---

* To whom correspondence should be addressed. Telephone: (803)-777-6018. Fax: (803)-777-9521. E-mail: myrick@psc.sc.edu.
† University of South Carolina.
‡ East Carolina University.
§ J. A. Woollam Company Inc.

(1) Aust, J. F.; Booksh, K. S.; Myrick, M. L. *Appl. Spectrosc.* **1996,** *50,* 382−387.
(2) Thomas, E. V.; Haaland, D. M. *Anal. Chem.* **1990,** *62,* 1091−1099.
(3) Ruyken, M. M. A.; Visser, J. A.; Smilde, A. K. *Anal. Chem.* **1995,** *67,* 2170−2179.
(4) Martens, H.; Naes, T. *Multivariate Calibration;* John Wiley & Sons: New York, 1989; Chapter 3.
(5) Nelson, M. P.; Aust, J. F.; Dobrowolski, J. A.; Verly, P. G.; Myrick, M. L. *Anal. Chem.* **1998,** *70,* 73−82.
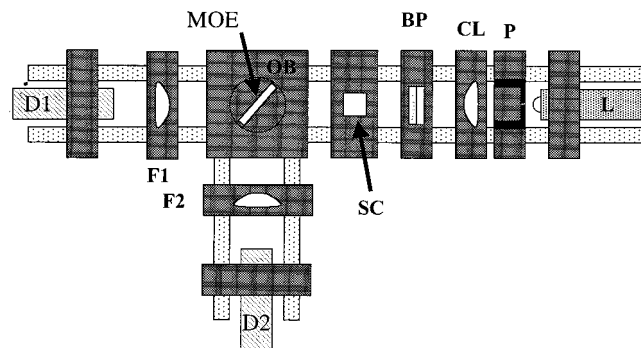(6) Bialkowski, S. *Anal. Chem.* **1986,** *58,* 2561−2563.

Figure 1. Schematic of a multivariate optical computing system for the measurement of BB in a binary dye mixture. Key: MOE, multivariate optical element; SC, quartz sample cell; OB, optical block; BP, band-pass filter set consisting of two 3-mm Schott glasses; CL, achromatic collimating lens; L, tungsten halogen lamp; P, pinhole; D1/D2, Si photodiode detectors for light radiation transmitted through and reflected from the MOE; F1/F2, focusing lens.

been described for the same purpose,[7] a permutation most similar to that proposed by Ryabenko and Kasparov.[8] The all-optical approach proposed by our laboratory differs from previous work by centering around the production of one or more optical interference coatings whose transmission spectra incorporate features of a spectral regression vector. Such interference filters based on multivariate spectroscopy will be referred to as MOEs. MOEs have never been demonstrated as a tool for actual chemical measurement, however.

This report details the first demonstration of multivariate optical computing (MOC) using an MOE. Simple binary dye mixtures of Bismarck Brown (BB) and Crystal Violet (CV) were selected to design a MOE that would test the concept of all-optical prediction. The experiments reported below consist of several elements. First, the optical properties of all the pertinent components of a simple T-format spectroscopic system were evaluated. Second, spectra of a series of binary dye mixtures were recorded and converted to a spectral radiance scale for chemometric interpretation. Third, a theoretical design for a MOE suitable to this measurement was generated. Fourth, the MOE was fabricated in-house. Finally, the MOE was installed in our T-format instrument and measurements of calibration and validation samples were performed.

EXPERIMENTAL SECTION

Owing to the possible confusion between dimensions for wavelength and layer thicknesses, in the following we will uniformly employ the units "nanometer" for dimensions of wavelength and "angstroms" for units of film thickness.

Demonstration of the MOC technique was carried out on a compact T-format instrument (Figure 1), which was constructed using Linos Photonics (Milford, MA) optical components.

A 6-V/6-W tungsten filament lamp (Linos Photonics) with 1 × 1.2 mm active filament area was used as a light source for the test instrument. The spectral radiance of the lamp was measured

in W/sr·cm²·nm with a CCD spectrometer system consisting of a Chromex 250IS spectrometer with a 300 line/mm grating blazed at 500 nm and a Princeton Instruments 1100 × 300 pixel CCD camera, model TE/CCD-1100-PE. The input optics on the spectrometer system were duplicates of the Figure 1 system. For these measurements, the operating voltage for the lamp was fixed at 5.76 V. The wavelength range of the camera/spectrometer system was calibrated with a standard mercury pen lamp and a standard neon lamp. The spectral radiance of the lamp under these conditions was calibrated against an OL series 455 integrating sphere calibration standard lamp (Optronic Laboratories Inc.) operated under standard conditions.

The two Si photodiode active detectors were type BPW21 (Linos Photonics) with a sensitive area of 2.7 mm², spectral range of 320−880 nm, and radiant sensitivity at the peak wavelength (550 nm) of 3.8 V/mW. The relative spectral sensitivity of the detector wavelength was estimated from a Linos Photonics data sheet giving values measured at 25 °C and 12-V dc supply voltage.

A band-pass filter set was used to isolate the spectral region between 400 and 650 nm in which the visible absorbances of the two dyes are found. The band-pass set consisted of two 3-mm-thick Schott glass filters (Duryea, PA) BG-39 and GG400.

Water-soluble dyes obtained from Aldrich Chemical Co. The dyes were Bismarck Brown (λ_{max} = 457 nm, dye content 50%) and Crystal Violet (λ_{max} = 590 nm, ACS reagent grade, dye content 95%). Stock solutions in distilled water of BB at a concentration of 82.3 μM and CV at a concentration of 37.7 μM were prepared.

Forty mixtures of BB and CV were prepared by dilution of the stock solutions in order to obtain data for multivariate calibration. These mixtures were made with known random concentrations of each dye to ensure that the concentrations of the two dyes were varied independently. The ranges over which the concentrations of BB and CV were varied were chosen to ensure that the minimum transmittance of the diluted mixtures in the 400−650-nm window were between 30 and 70%. BB was selected as the analyte because the spectrum of CV was an interference at all wavelengths over which BB absorbed. CV was treated as an uncorrelated interference. Optical spectra were recorded on a Hewlett-Packard UV−visible diode array spectrometer (model 8543). The samples were measured in a 1-cm fused-silica cell (Starna Cells Inc., Atascadero, CA).

Following data collection and radiometric corrections for lamp intensity, detector response, and band-pass, design of MOE coatings was performed in two different ways. First, a spectral vector based on a principal components regression (PCR) model with four components was defined, and an iterative spectral-matching synthesis was performed. This procedure used TFCalc, a commercial software product from Software Spectra, Inc. (Portland, OR). The second approach began by synthesizing a crude filter design based on spectral matching to the PCR vector. The result of the crude spectral match was then used to initialize a nonlinear least-squares optimization routine to produce the final filter design.[9] The nonlinear least-squares algorithm was written in-house in the MATLAB programming environment. More detail is provided in the discussion below.

(7)   Myrick, M. L. Soyemi, O.; Karunamuni, J.; Eastwood, D.; Li, H.; Zhang, L.; Gemperline, P. *Vib. Spectrosc.,* in press.
(8)   Ryabenko, A.; Kasparov, V. *Pattern Recognit. Image Anal.* **1991**, *1*, 347−354.

(9)   Soyemi, O.; Gemperline, P. J.; Zhang, L.; Eastwood, D.; Li, H.; Myrick, M. L., in preparation.
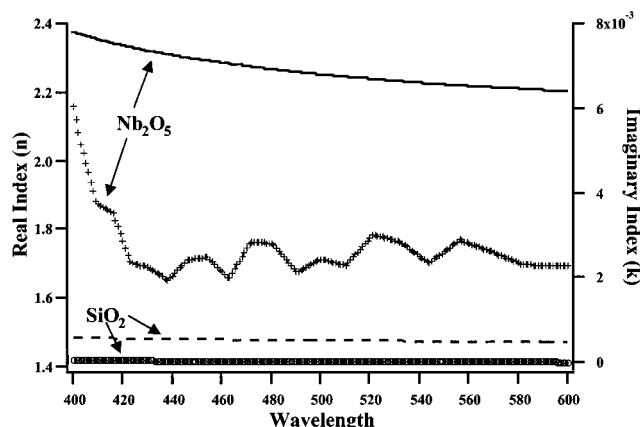
Figure 2. Real refractive indices of Nb_2O_5 (solid line) and SiO_2 (dashed line) deposited in the USC deposition chamber in the wavelength region between 400 and 600 nm as determined from variable-angle spectroscopic ellipsometry. The left axis gives values for real indices. Imaginary refractive indices are indicated by + (Nb_2O_5) and o (SiO_2) on the right axis.

The MOE was manufactured via reactive magnetron sputtering (RMS). Our sputtering system (model CV 5.1) was custom-manufactured by Corona Vacuum Coaters of Vancouver, BC. The system operates at room temperature and utilizes a 40-kHz midfrequency rf supply to power four water-cooled planar magnetrons positioned in pairs around a drum that rotates about a horizontal axis. The coating chamber is 55.9 cm in diameter and 50.8 cm deep and contains 10.1 cm × 25.4 cm magnetron targets, two containing niobium (99.95% pure, high index) and two containing silicon (99.9999% pure, low index). Each magnetron target is powered at ~0.7 kW, although the power is varied during deposition as one method of controlling deposition rate. The RMS process was used to deposit alternating layers of niobium pentoxide and silicon dioxide films by reaction with oxygen in the gas mixture. MOE designs require accurate knowledge of the optical constants of the coating materials. Figure 2 shows experimental measurements of the real and imaginary refractive indices of Nb_2O_5 and SiO_2 deposited in our chamber as determined by variable-angle spectroscopic ellipsometry.

The MOE tested here was fabricated on a 2.54-cm BK-7 glass substrate. Layer deposition was optically monitored on-line with a 1200 line/mm grating monochromator (model 9030, Sciencetec, London, ON, Canada) blazed at 250 nm. Light detection was achieved using a photomultiplier tube (model H5784-03, Hamamatsu, Japan). Visible light was obtained from a tungsten filament lamp (Gilway Technical Lamps, Waltham, MA). After MOE design was completed, the interference effects on transmission for each layer were computed at all accessible monitoring wavelengths. The system can currently monitor wavelengths between 420 and 600 nm with ~1-nm resolution, and thus ~180 different "monitor curves" were produced for each layer. From the 180 possible curves, the optimum wavelength for monitoring and controlling the deposition of each layer was selected based on a set of criteria developed as a result of experience in our laboratory. Process control of the deposition process was performed with in-house software written in the LabVIEW 5.1 programming environment that operated in concert with the system control software provided by Corona Vacuum Coaters. The two software packages used the

selected monitor curves to deposit each filter layer as accurately as possible. More detail is provided in the discussion below.

After the production of the MOE as described above, it was installed in the T-format instrument shown in Figure 1. A total of 39 new samples of BB and CV were prepared using the random number generation described above. The difference between the signal due to light transmission through the sample followed by transmission through the optical filter (aligned at ~45°) and light transmission through the sample followed by reflection from the surface of the optical filter was measured for each sample. Twenty of these measurements were used for calibrating the instrument (determining the optimum relative gain factor for the two detectors, vide infra), while the remaining 19 samples were used to validate the calibration model.

The relative gain factor described above is used to correct for the fact that the two detectors illustrated in Figure 1 have slightly different responsivities. These different responsivities can result from variance in the electronics of the two detectors or from other causes. When performing calculations using two detectors in our setup, we used a set of calibration samples to obtain measurements of transmittance and reflectance and then varied an empirical relative gain factor (called K in the discussion below) until the best correlation was obtained. This optimum gain factor was then used for future experiments.

RESULTS AND DISCUSSION

Single MOEs can be designed for chemometric prediction by using them in a beam splitter arrangement as shown in Figure 1.[7] Consider the optical transmission spectrum of an MOE to be $T(\lambda) = 0.5 + L(\lambda)$, where $L(\lambda)$ is a spectral pattern that can also be represented in vector form as $\mathbf{l}$. Assuming negligible absorbance in the MOE, the difference between the intensity of light transmitted through the MOE ($\mathbf{t} \cdot \mathbf{x}_i$) and light reflected from it ($\mathbf{r} \cdot \mathbf{x}_i$) is proportional to the scalar product of the vector $\mathbf{l}$ with the sample spectrum vector for the ith sample, $\mathbf{x}_i$

$$\mathbf{t} \cdot \mathbf{x}_i - \mathbf{r} \cdot \mathbf{x}_i = (\mathbf{t} - \mathbf{r}) \cdot \mathbf{x}_i =$$
$$((0.5 + \mathbf{l}) - (0.5 - \mathbf{l})) \cdot \mathbf{x}_i = \mathbf{l} \cdot \mathbf{x}_i \quad (1)$$

In this measurement paradigm, $\mathbf{l}$ can be chosen to be proportional to a regression vector for a dependent sample variable. Because an MOE must have transmittance values between 0 and 1 inclusive, $\mathbf{l}$ can have a magnitude no greater than 0.5 at any wavelength. For reasons of improving signal-to-noise ratio, the magnitude of $\mathbf{l}$ should be made as large as possible, subject to this limitation. Thus, the scalar product of this vector with the spectral vector is proportional to the value of the dependent variable ($\hat{y}_i$), with a proportionality constant we will represent by G/m (where m is the number of wavelength channels in the vectors) and an offset (off):

$$\hat{y}_i = (G/m)(\mathbf{l} \cdot \mathbf{x}_i) + \text{off} \quad (2)$$

To achieve this, the spectrum of the 45° filter (the MOE in Figure 1) must be designed such that an optimal multivariate regression vector can be derived from it that results in the best possible standard error of sample prediction (SEP). This regression vector, according to equation two, is the vector $\mathbf{R} = (G/m)\mathbf{l}$.

1. Selection of the Spectral Window and Spectral Mode.

Although MOC should function in many linear types of spectroscopy, the most convenient and most basic multivariate measurement to set up is spectral absorbance. MOC should also function in any spectral range where good optical elements can be produced. However, in our laboratory, our experimental system lends itself most conveniently to measurements in the visible spectroscopic region. This is because our MOE fabrication system is presently process-controlled using an optical monitor between 420 and 600 nm. We elected to make measurements of mixtures of visible-absorbing dyes in the spectral window between approximately 420 and 600 nm.

Absorbance is nominally linear in concentration within the limits over which Beer's law holds. A radiometric measurement, however, is more directly related to transmittance of the sample than absorbance, and transmittance is logarithmically related to concentration. Nevertheless, a number of studies correlating single-beam and radiometric measurements to chemical properties using linear chemometric models have been performed with some success.[10,11] In the limit of low absorbances, transmittance varies linearly with concentration; even for high absorbances, transmittance can be considered piecewise linear with concentration. Also, it has been shown that linear multivariate calibration methods such as PCR and partial least-squares regression (PLS) can satisfactorily model nonlinear responses by the inclusion of extra factors or latent variables in the calibration model.[12] In the following discussion, the raw data from which an MOE is designed will be analyzed in both transmittance and absorbance modes for comparison purposes to evaluate how the nonlinearity of transmittance with concentration affects the resulting prediction error.

Since measurement by an MOE-based instrument is inherently radiometric in nature, a number of factors not normally considered in absorption measurements must be quantitatively evaluated. These include the following: (a) the spectral radiance of the source, (b) the transmittance of the samples, (c) the transmittance of any band-pass-selection filter, (d) the spectral sensitivity of the detector, and (e) the determination of the effective band-pass. Once these factors are known, the design of an MOE must be conducted via iterative thin-film synthesis subject to suitable starting, optimization, and stopping criteria. Following thin-film design, the precision of the fabrication process must be extreme. This requires a real-time monitoring system with suitable control software and accurate knowledge of the optical constants of materials involved in fabrication. Only after all these issues have been dealt with and concluded satisfactorily can the final system be evaluated. The following sections describe each of these basic considerations in detail.

2. Radiometric Correction of Spectral Data.

A realistic representation of the MOC instrument detector signal must include a convolution of the following radiometric quantities: the detector sensitivity, the spectral radiance of the source, the spectral band-pass, and the sample transmittance, all of which are functions of wavelength. Figure 3 shows the transmittance spectra of 40 mixtures of the two dyes in the region between 400 and 650
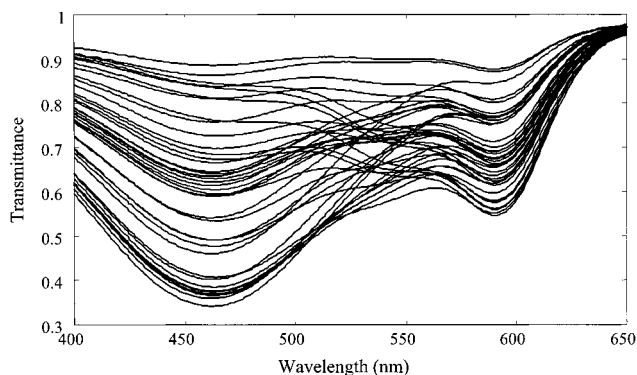

Figure 3. Transmittance spectra of 40 binary mixtures of Bismarck Brown and Crystal Violet acquired on a UV–visible diode array spectrometer.

nm (with concentration and wavelength ranges similar to those described above).

In ordinary chemometric applications, out-of-band light can be eliminated by simply ignoring it. That is, light from the sample that is not in the range over which the chemometrics is performed does not have to be sampled. In the MOC measurement, however, band selection filters must be used to obtain this result. To ensure that light from outside the wavelength range of our targeted response window is not transmitted through the MOE onto the detector, a colored-glass band-pass filter set whose transmittance profile is shown in Figure 4A was used.

Si photodiode detectors were selected for the dual-channel measurement system (Figure 1). Figure 4B shows a plot of the detector spectral sensitivity versus wavelength as estimated from a manufacturer-provided graph. The sensitivity reaches a maximum at ~550 nm and tapers off in the short-wavelength near-infrared region (not shown in the figure).

A tungsten filament lamp was selected to serve as a light source for the measurement. These lamps are approximately blackbody-type emitters, with a spectral radiance maximum in the near-infrared. Figure 4C shows the spectral flux (in W/nm) of our tungsten filament lamp after passing through a 1-mm pinhole. The spectral flux profile was obtained by correcting the measured spectral radiance profile for the active solid angle ($=(3/4)(r^2/f^2)$) sr, where r and f are the radius and focal length of the focusing lens in the calibration system, respectively) and the active pinhole area ($=\pi r_p^2$, where r_p is the radius of the pinhole).

Figure 4D shows the sample transmittance spectra corrected for the radiometric quantities described above, and they represent the spectral signal for each sample.

3. MOE Design.

An initial permutation of the MOC technique was proposed which involved the reproduction of the positive and negative lobes of the PCR regression vector on two separate filter elements.[5] In this original conception, the light transmitted through two MOEs is separately detected to give a difference signal that is proportional to the sample concentration. The MOC configuration used in the study requires only a single MOE in a T-format configuration in which the MOE acts as a 45° beam splitter. Because of this, the MOE is designed to operate at this angle. Coatings at nonnormal incidence are prone to strong polarization effects. However, our calculations assumed completely unpolarized light since the light source for the instrument is an on-axis tungsten lamp. The algorithm thus designs a coating for

(10) Ding, Q.; Small, G. W.; Arnold, M. A. *Appl. Spectrosc.* **1999**, *53*, 402−414.

(11) Hazen, K. H.; Arnold, M. A.; Small, G. W. *Anal. Chim. Acta* **1998**, *371*, 255−267.

(12) Gemperline, P. J.; Long, J. R.; Gregoriou, V. G. *Anal. Chem.* **1991**, *63*, 2313−2323.
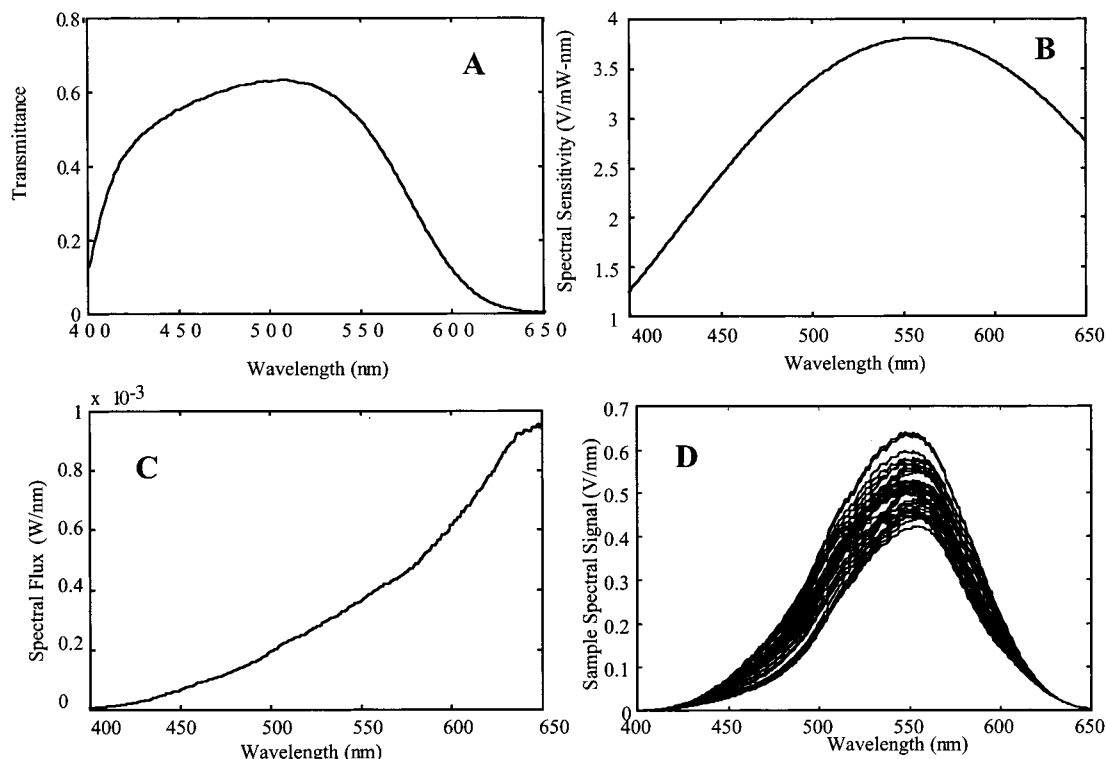
Figure 4. (A)−(C) are the characteristics of selected radiometric quantities for the T-format measurement system in Figure 1: (A) Band-pass of two 3-mm Schott glass filters versus wavelength, (B) detector sensitivity of two Si photodiode detectors versus wavelength, and (C) source radiance of the tungsten filament lamp versus wavelength. (d) shows the sample spectra in Figure 3 corrected for the three radiometric quantities in (A)−(C).

light with equal magnitudes of *s*- and *p*-polarized light; our unpolarized light source provides such light to a very good approximation as long as the lamp is on the optical axis of the system. For the same reason, the detectors must be kept on axis as well.

The corrected detector response profiles (corrected transmittance spectra) in Figure 4D were used for MOE design. Two possibilities exist for designing a viable MOE, both of which use iterative solving approaches. In each, calculation of the MOE spectrum from the design utilizes a matrix formulation that is based on the solutions to Maxwell's equations.[13] The spectrum of a hypothetical coating is obtained and then evaluated subject to various criteria and then modified in ways that improve the criteria for evaluation. The criteria are the main points of differentiation between the two methods for design we will describe below. The first entails the transfer of the structure of a PCR regression vector onto a filter element via spectral matching using the established needle optimization technique.[14−16] The evaluation criteria in this case are "goodness of spectral match". The second method of MOE design referred to in the Experimental Section above uses a novel algorithm that synthesizes the best filter solution based on the constraint of minimizing standard error in sample prediction.

Effective Band-Pass. As Figure 4A shows, the band-pass defined by our colored-glass filters is not clear-cut. The transmission band of the filters is far from a rectangular function of wavelength. An operational definition of the band-pass can be proposed, however, as the wavelength range over which the transmittance function of the MOE must be defined. In other words, outside the operational band-pass, all values of transmittance for the MOE are permissible because the variance of the signal strength is so small that it has a negligible impact on prediction. Determination of the operational band-pass limits has recently been examined in a discussion of spectral tolerance for MOE design.[17] The lower and upper wavelength limits of the spectral band are given by solving the following equation:

$$V_{ex} = V_{co}(\lambda_R - \lambda_L) - \frac{SEP^2}{2(G/m)} = 0 \qquad (3)$$

where V_{ex} is the excluded variance of the spectroscopic samples at all wavelengths outside the band-pass, V_{co} is the variance cutoff value at wavelengths defining the edges of the band-pass, λ_R and λ_L are the right and left wavelength limits of the band, SEP is the standard error of prediction for the calibration model, and (G/m) is the proportionality factor defined in eq 2. Based on the original 40-sample calibration set, the effective band-pass was determined to be between 424 and 622 nm for these data.

Spectrum Matching. Reference 5 describes needle optimization as a method by which spectral transmission targets can be

(13) Liddell, H. M. *Computer-Aided Techniques for the Design of Multilayer Filters*; Adam Hilger Ltd.: Bristol, U.K., 1983; Chapter 1.
(14) Dobrowolski, J. A.; Lowe, D. *Appl. Opt.* **1978**, *17*, 3039−3050.
(15) Tikhonravov, A. V. *Vest. Mosk. University, Ser 3: Fiz., Astron.* **1982**, *23*, 91−93.
(16) Verly, P. G.; Tikhonravov, A. V.; Trubetskov, M. K. *Appl. Opt.* **1997**, *36*, 1487−1495.
(17) Myrick, M. L.; Soyemi, O.; Li, H.; Zhang, L.; Eastwood, D. *Fresenius J. Anal. Chem.* **2001**, *369*, 351−5.
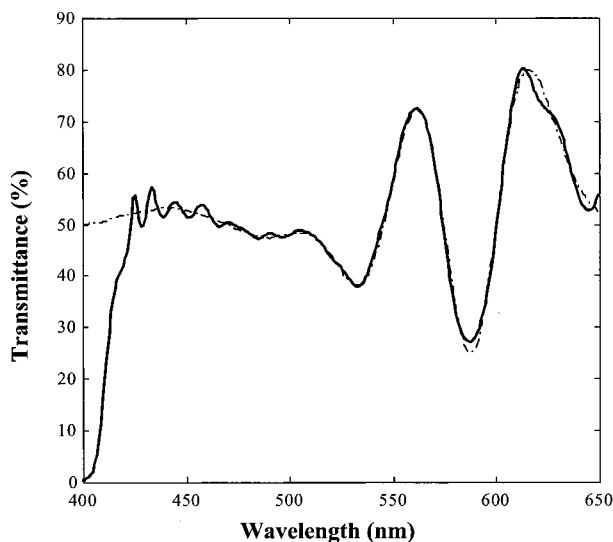
Figure 5. Comparison of the spectral target generated from the 4-factor PCR regression vector for the determination of BB generated from a calibration set of 20 binary dye transmittance spectra (dashed line), to the transmittance spectrum of a MOE designed by spectral matching with permissible tolerances (solid line).

approximated through iterative synthesis of an interference coating.[15] It is the basis for several commercial thin-film design programs that are presently available.[18,19] Using needle optimization, the MOE design that best matches the spectral profile of the PCR vector is iteratively synthesized by minimizing a merit function, F, which describes the difference between a calculated spectrum (based on the MOE layer thicknesses in each iteration) and the target spectrum (represented by the spectral profile of the PCR vector). F for a spectral-matching synthesis routine can be defined by

$$F = \left(\frac{1}{m} \sum_{j=1}^{m} \frac{|Z_j^D - Z_j|^k}{\text{Tol}_j} \right)^{1/k} \qquad (4)$$

where Z_j^D is the calculated response (e.g., transmittance) value at wavelength j, Z_j is the target value, Tol_j is the design tolerance at that wavelength, m is the number of wavelength targets, and k is an algorithm gain factor used to weight the relative importance of mismatched regions. Design tolerances can be selected for each wavelength channel, which specify the minimum allowable deviation from the target at that wavelength. The design process involves the insertion of a zero-thickness layer (needle) into the MOE refractive index profile at each iteration of the optimization routine. The insertion results in the adjustment of existing layer thicknesses as well as that of the new layer to give a better (lower) estimate of the merit function. The process continues until the merit function can no longer be minimized. The periodic application of a "tunneling" function helps in achieving a global minimum for the optimization process by regularly perturbing the system as a means of escaping local minimums. Figure 5 shows a comparison of the transmittance spectrum of a MOE element

(18) TFCalc, Software Spectra Inc., Portland, OR.
(19) FilmWizard, Scientific Products and Services Inc., Carlsbad, CA.

produced by spectral matching to the target spectrum. The target spectrum was created from the 4-factor PCR regression vector that resulted from the calibration of 20 binary dye detector profiles with corresponding BB concentrations. Although the spectrum (the solid line in Figure 5) varies from the target (the dashed line) in some wavelength regions, the result is within the allowable tolerances for the design. The main complication of this approach to designing MOEs is that the PCR regression vector is not necessarily the basis for the simplest MOE.

For example, this MOE designed by spectral matching using spectral tolerances determined as reported elsewhere[17] consists of 46 alternating layers of Nb_2O_5 and SiO_2, with a total coating thickness of 3.7 μm. The deposition system we use for depositing these coatings (vide infra) would require ∼2 days to produce this coating. Further, the accuracy with which a spectrum can be created in an actual MOE is related to the number of layers in the coating; more layers provide increased opportunity for manufacturing errors. The MOE designed by spectral matching was not fabricated. Instead, we pursued an alternative method to MOE design developed in our laboratory with the aid of P.G. Conceptually, this new approach could be called "spectral vector relaxation" (SVR). The basis for SVR is that many vectors satisfy the criteria for good regression vectors in addition to the ones that are found via PCR. Some of these vectors will be easier to fabricate in the MOE form than others; we seek a general method for locating those that are the simplest to fabricate.

MOE Design via Least-Squares Minimization of Sample Prediction Error: SVR. Even with the careful selection of design tolerances, there is no guarantee that needle optimization will produce a design that matches a spectral target *and* can be readily fabricated. For example, in cases where the target spectrum has many high-frequency components (e.g., noise), it is quite likely that a MOE design will result with many layers and a large value of total layer thickness. Such coatings are difficult to fabricate using conventional thin-film deposition techniques because manufacturing errors accumulate with each layer and because stress builds between the coating and its substrate with increasing coating thickness. Such stress will generally lead to coating delamination when the coating thickness exceeds ∼10−25 μm. In addition, economic considerations of long deposition cycles argue for simplified, thinner coatings.

Instead of trying to match a PCR regression that represents a fixed SEP, an alternative algorithm has been developed that combines design with optimization of the SEP.[9] This algorithm is based on a nonlinear least-squares optimization technique and attempts to synthesize the optimum MOE design at a given level of complexity of the coating. In other words, instead of creating an MOE design whose spectrum matches a regression vector, an MOE design is created with a fixed upper-bound level of complexity (numbers of layers and layer thicknesses). Among all the possible MOE designs with a fixed maximum level of complexity, the one whose spectral profile results in an optimal value of the SEP can then be obtained.

Unlike the previous design method, which starts from a single layer and gradually builds up the coating, the SVR filter design algorithms are initialized with a specified number of layers with either random or predetermined layer thicknesses.

Table 1. 26-Layer MOE Design for the Determination of Bismarck Brown in a Binary Dye Mixture with Crystal Violet Showing the Individual Layer Thicknesses (in Nanometers)[a]

layer no.	material	layer thickness (Å)	layer no.	material	layer thickness (Å)
1	Nb_2O_5	279	14	Nb_2O_5	675
2	SiO_2	2099	15	SiO_2	374
3	Nb_2O_5	702	16	Nb_2O_5	675
4	SiO_2	796	17	SiO_2	493
5	Nb_2O_5	477	18	Nb_2O_5	795
6	SiO_2	657	19	SiO_2	309
7	Nb_2O_5	434	20	Nb_2O_5	2024
8	SiO_2	723	21	SiO_2	1023
9	Nb_2O_5	328	22	Nb_2O_5	796
10	SiO_2	664	23	SiO_2	1539
11	Nb_2O_5	304	24	Nb_2O_5	921
12	SiO_2	1405	25	SiO_2	881
13	Nb_2O_5	577	26	Nb_2O_5	720

[a] Layer 1 is the layer closest to the substrate (BK-7 optical glass).

If n is the number of layers in the coating, optimization using the SVR algorithm can be visualized in an $n + 2$ dimensional space. The additional two dimensions in the space are scaling (G/m) and offset (off) factors relating the spectral vector to the dependent variable in the sample. The figure of merit in this optimization is the SEP for prediction of the dependent variable using the design of the coating at each iteration. The steps to calculating the SEP at the end of each iteration is as follows; first, the current optical transmission spectrum ($T(\lambda)$) spanning m wavelength channels is scaled to a regression vector ($\mathbf{R}$) as in

$$\mathbf{R} = (G/m)[2\mathbf{t} - 1] \qquad (5)$$

Next, an estimate of the concentration of sample i ($\hat{y}_i$) is determined as the offset scalar product of its spectrum ($\mathbf{x}_i$) with the regression vector ($\mathbf{R}$), where t represents the vector transpose.

$$\hat{y}_i = \mathbf{x}_i \mathbf{R}^t + \text{off} \qquad (6)$$

By substituting eq 5 into eq 6, the SEP for N validation samples is calculated thus:

$$\text{SEP} = \frac{\sum_{i=1}^{N}\left\{\left\{\mathbf{x}_i\left[\frac{G(2\mathbf{t}-1)}{m}\right]^t + \text{off}\right\} - y_i\right\}^2}{N} \qquad (7)$$

During optimization, layer thicknesses that fall below a specified threshold value are deleted because extremely thin layers are difficult to deposit accurately in our current apparatus. Because the final MOE design that results from SVR can have less than, or equal to, the starting number, this novel algorithm creates designs with smaller overall coating thicknesses than those created with needle optimization. In practice, we have found that this can often be achieved without sacrificing predictive ability.

The starting point of the optimization routine is important since the SVR algorithm can converge to a nonglobal optimum. The choice of an appropriate starting point usually produces a rapid descent to the global optimum for a given upper-bound level of complexity.
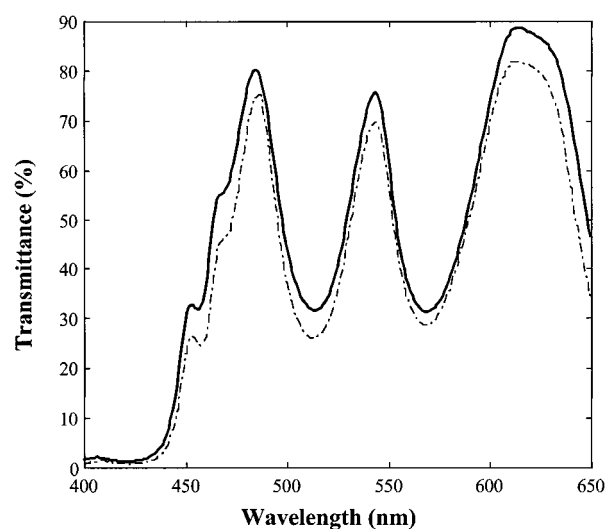

Figure 6. Results for a MOE produced by SVR. Comparison of the measured MOE spectrum at 45° (dashed line) to the calculated SVR MOE spectrum at 45° (solid line). Polarization effects in the measured spectrum are uncorrected.

There are currently two variants of the SVR MOE design algorithm that differ in their modes of initialization. The first one initializes the optimization process with a specified number of layers with random thicknesses, which are then modified to give the best MOE design. Starting with a random number of layers or layers with fixed thicknesses, the second variant to the design algorithm creates a partial design by crudely matching the PCR regression vector using standard spectral matching. With this partial design as the starting point, the MOE spectrum is then further refined. The SVR approach does not add new layers but instead deletes layers that fall below a specified minimum permissible thickness during iteration. For comparison to the 46-layer spectral-matching design described above, we initialized a SVR design beginning from a partial needle design consisting of 30 layers. The final SVR result is shown in Table 1. This design, which corresponds to an SEP of 0.31 μM, has 26 layers with total thickness of 2.1 μm (solid line in Figure 6) and was selected for fabrication and testing, as described in the following sections.

4. MOE Fabrication. The multilayer thin-film coating as synthesized by the filter design algorithm consists of alternating layers of Nb_2O_5 and SiO_2 deposited on a glass substrate (Corning

BK-7). These materials have well-defined refractive indices as shown in Figure 2 and are suitable for use between the near-UV and the long-wavelength mid-infrared spectral regions. Only one set of targets, either of elemental niobium or elemental silicon, is operated at a given time during deposition, producing films of exclusively one or the other material.

During the RMS process,[20] argon atoms are ionized and entrained in a magnetic field. The argon ions strike the elemental targets and eject atoms from the targets by momentum transfer. Oxide films form on the substrate as a result of the reaction of the metal atoms and oxygen in the chamber gas. This reaction occurs exclusively on the substrate under the conditions of deposition. The placement of the substrate on a 35.6-cm-diameter octagon-shaped rotating drum ensures a uniform coating as the drum sweeps through the deposition zone.

Process Control. The layer thicknesses of the coating materials must be controlled very precisely during deposition to ensure that the MOE spectrum accurately matches the design. The progress of the MOE fabrication is optically monitored by keeping track of the evolving filter spectrum as each layer is deposited. This is done with monitor curves, which are single-wavelength transmittance spectra of the evolving MOE spectrum for individual layers (i.e., transmittance versus layer thickness). In an ideal situation, experimentally measured monitor curves are compared with calculated values to determine the end point of layer deposition. The facilities that are currently available to us for process monitoring do not allow us to directly measure the true transmittance as the layers are coated, but instead only the power transmitted through the coating. The relationship between the observed monitor values and the predicted monitor curves is found by normalizing the experimental monitor curves to the theoretical curves at turning points in their transmission as a function of layer thickness. Layer deposition is terminated when normalized values of the transmittance match the value expected for the target thickness as closely as possible. In our experience, the fairly complex normalization routines we have built into our LabVIEW process control engine only work well when the monitor curve wavelengths are selected subject to the following criteria:

(1) The monitor curve should have adequate curvature with well-defined maximums or minimums. This is because maximums and minimums provide the most stable points for normalization of the experimental transmitted power measurements to the predicted transmittance monitor curves.

(2) The monitor curve should cover a fairly wide range in transmittance values because the rate of transmittance change per unit deposition thickness is directly related to the precision with which the layer can be deposited.

(3) Slight changes in the monitor wavelength should not result in rapid changes in either the shape of the monitor curve or the range in transmittance values that are covered by the monitor curve. This is because errors inevitably accumulate, shifting the monitor curves to higher or lower wavelengths by small amounts. Monitor wavelengths at which the monitor curves experience large changes with small errors in wavelength lead to irreproducible results and frequently to serious errors in fabrication.

(20) Parsons, R. Sputter Deposition Processes. In *Thin Film Processes;* Vossen, J. L., Kern, K., Eds.; Academic Press: San Diego, 1991.

As an example, Figure 7 shows the calculated (transmittance versus physical thickness) and experimental (transmitted power versus number of deposition cycles) monitor curves for the first 2 layers of the 26-layer SVR MOE. Deposition is closely monitored by matching the two curves for each layer. The two layers correspond to a total thickness of 2400 Å. After the selection of appropriate monitor curves, the software program generates a recipe file which contains the chamber operating conditions for the initial deposition of all the individual layers. Since these conditions are based purely on the approximate deposition rate of the materials, they are only accurate to within about ±5%. Consequently, the system is designed to automatically deposit only 80% of each layer initially to avoid overdepositing the layer before the process control algorithm comes into play. The parameters entered into the recipe file include the Ar and O_2 flow rates (controlled by mass flow controllers), predetermined monitor wavelengths for each layer, the number of deposition cycles required for ~80% deposition of each layer, the magnetron power, predeposition sputtering time (to clean the targets of contaminants), and the detector gain. After each layer is 80% deposited, new commands are entered into the recipe file by our process control engine to make adjustments to the process parameters until the layer deposition is complete. These updates to the recipe file are fully automated. The experimental curves, particularly for the first layer (Figure 7B), do not appear to faithfully reproduce the theoretical curve. This is only due to the operation of the process control engine, which adjusts the rate of deposition so that the final layer thickness is achieved as nearly as possible. This gives the experimental measurements a "stuttered" appearance as the process control engine iterates to a physical end point.

Deposition rates are rarely constant due to slight fluctuations in power as well as the values of the optical constants (i.e., layer absorption coefficients and refractive indices as functions of wavelength) of the two materials at room temperature over a period of time. Also certain layers are more sensitive to errors than others due to a lack of adequate monitor curves at the available wavelengths. These factors combine to introduce minor errors in the MOE spectrum. Despite this, we have been able to routinely produce filter elements with better than 95% accuracy. Figure 6 shows a comparison of the measured MOE spectrum at 45° to the design (theoretical) spectrum. Much of the error between the two curves is an offset due to polarization in the spectrometer that recorded the measurement. Even so, there is a reasonably good fit between the two spectra.

5. Installation and Tuning of the MOE in the Measurement System. The optical spectra of the original samples from which the MOE was designed were recorded on a UV−visible diode array spectrometer. However, the deposition of the coating is controlled with a different spectrometer. If these two spectrometers are not exactly calibrated in wavelength with one another, the result will approximately be a fixed wavelength offset between the actual MOE spectrum at the desired angle of incidence and the designed MOE spectrum at the same angle. Provided that this error is small, it can be corrected by slightly tuning the angle of the MOE in the measurement system. That is, instead of using the MOE at exactly 45°, the optimum angle might be slightly more or less than 45°, depending on the wavelength calibrations of the two spectrometers. The best spectrometer for making this
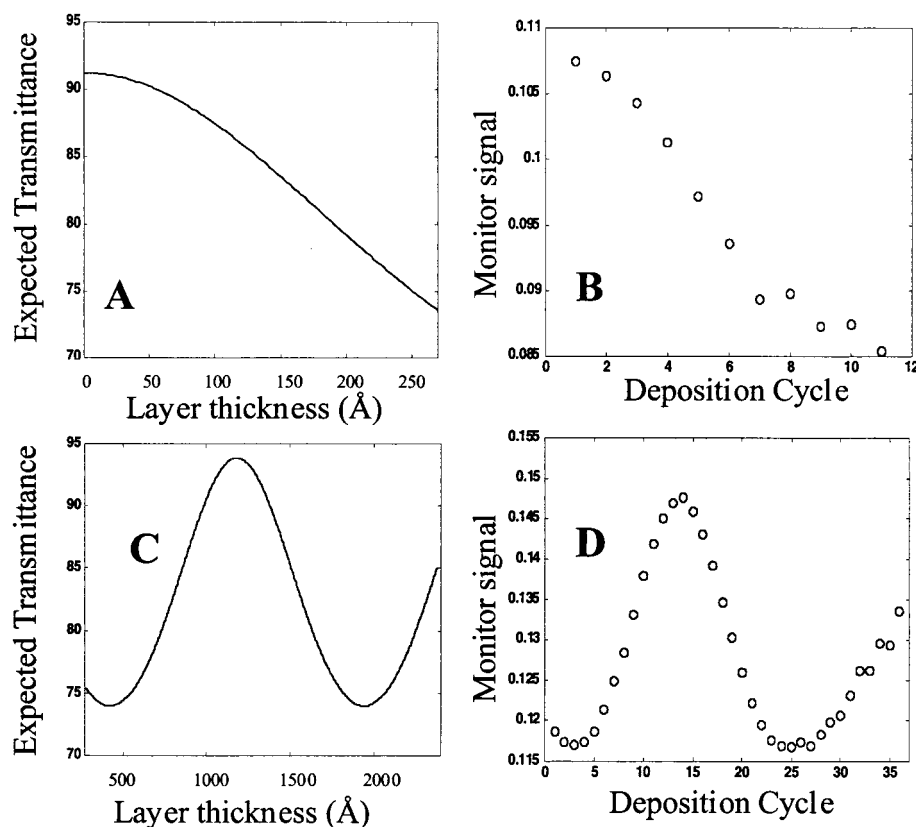
Figure 7. Theoretical and experimental monitor curves for layers 1 and 2. (A) Theoretical layer 1 monitor at 420 nm; (B) experimental layer 1 monitor at 420 nm; (C) theoretical layer 2 monitor at 450 nm; (D) experimental layer 2 monitor at 450 nm.

determination is clearly the one on which the original samples were measured. For this reason, a device to adjust the filter angle prior to sample measurements was built. This device consists of a micrometer-driven adjustment for the MOE angle. When the MOE was installed in the optical block shown in Figure 1, the optical block was transferred to the original spectrometer and adjusted with the micrometer-driven tool to match the wavelength axis with the design as closely as possible. After adjustment, the MOE was locked in place and transferred back to the optical system for measurements.

6. Analysis of Crystal Violet/Bismarck Brown Dye Mixtures. *Conventional PCR Regression on Absorbance and Transmittance Data.* To gauge the results of the MOC measurements (using the apparatus in Figure 1 fitted with the fabricated MOE) against conventional multivariate calibration, conventional PCR regression analysis was carried out on the same data set used for MOE design. A PCR calibration of the BB concentration (requiring two factors) was initially carried out with absorbance spectra that are obtained by the conversion of the measured transmittance spectra ($A = -\log T$). This produced a SEP of 0.2 μM in BB. Next, a PCR calibration (requiring four factors) was done with the corrected detector intensity response. Despite the nonlinearity between the detector response and concentration, a linear calibration was obtained with an SEP of 0.26 μM. This is slightly worse than the results obtained from calibrating the absorbance spectra; nevertheless, the results are reasonably comparable as shown in Figure 8. The corresponding SEP for the radiometrically corrected spectra and our theoretical 26-layer MOE is slightly higher at 0.31 μM.
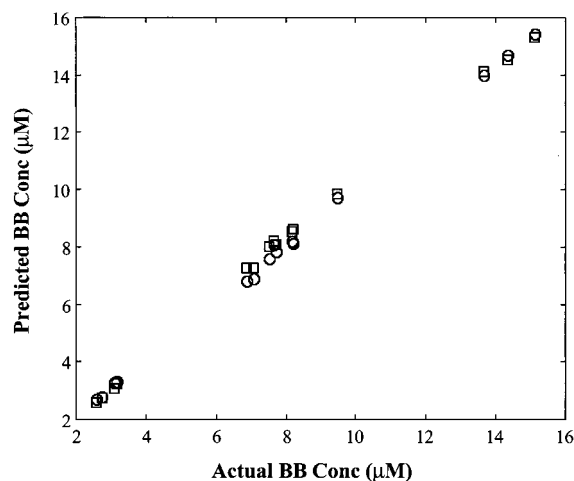

Figure 8. Calibration in absorbance vs transmittance modes. Comparison of PCR calibration of BB in a binary dye mixture using absorbance spectra (squares) with PCR calibration using radiometrically corrected transmittance spectra (circles).

Expectations versus Realities. The theoretical SEP for our 26-layer SVR MOE is based on spectra obtained on a conventional spectrometer. To evaluate the way in which a real MOE will operate, we should consider the source of the SEP. If, for instance, 0.31 μM is an SEP attributable to model or reference errors (as is probably the case here), then a real MOE-based device could produce an actual SEP no better than this value. In other words, if model or reference errors are responsible for the SEP, then the theoretical (model) SEP is a lower bound for the real SEP. Errors in the production of the MOE or errors in the calculations
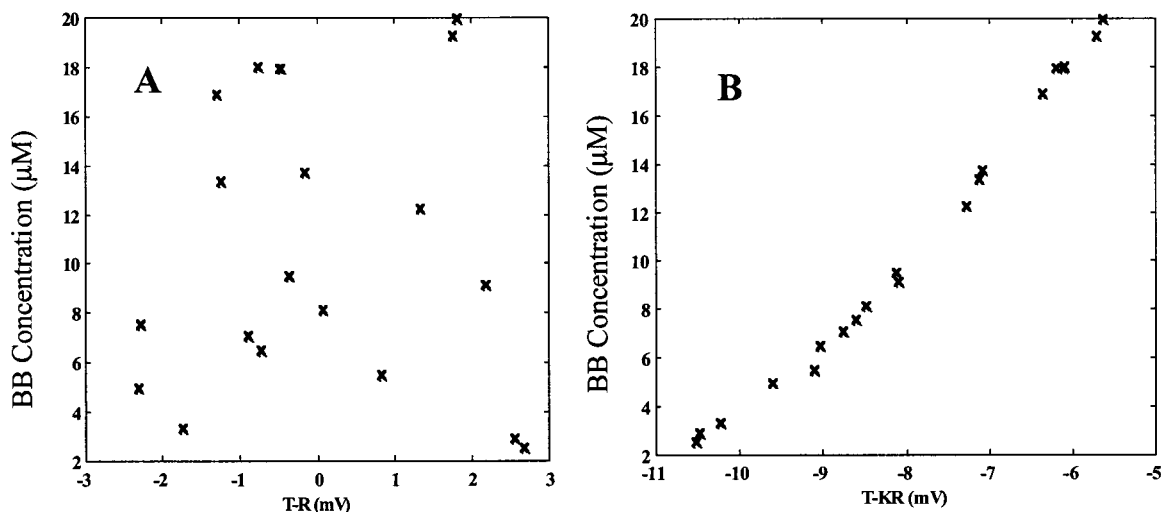
Figure 9. Effect of the detector relative gain factor. $T - KR$ vs the calibrated concentration of BB with unscaled vs optimized scaled detector sensitivities. T and R are the measured transmitted and reflected intensities, respectively, and K is the relative gain factor. (A) $K = 1$. (B) $K = 1.18$ (optimum).

preceding the model could negatively impact the result but probably not improve it. On the other hand, if the SEP is not limited by model or reference error but by signal-to-noise ratio in the original measurements on conventional instruments, an MOE could conceivably improve the result. As described in ref 5, MOEs are far less sensitive to detector noise contributions and low light levels than are conventional spectrometry systems. In general, UV−visible spectroscopy and modeling is not limited by noise but by model or reference errors. Thus, we should anticipate that our actual MOE will not miraculously reduce the expected SEP.

Determination of Bismarck Brown with the MOC Approach. The difference (in millivolts) in detector signals between detectors viewing MOE-reflected versus MOE-transmitted light that first passed through validation samples was measured for 39 samples. These samples were different from those samples that were used for MOE design, but were designed with a similar spread of concentration values. A total of 20 of these samples were used to evaluate the relative responsivities (the relative gain factor) of the two detection arms of the measurement system. To understand why this is necessary, consider that the two detectors shown in Figure 1 are physically different devices and thus can have slightly different relative responses. Since the MOC measurement is given by the difference in the two detector responses, a correction factor is necessary to give them the same overall gain. If this relative gain factor is called K, to ignore it assumes $K \approx 1$. Figure 9A shows the result of ignoring K. With an incorrect value of K, correlation between the detector differences and the BB concentration is seriously degraded. Figure 9B shows the optimum correlation obtained between the detector differences and BB concentration by giving $K = 1.18$ in the MOC equation,

$$C = 3.64 \, (T - KR) + 39.57 \qquad (8)$$

where C is BB concentration in micromolar and T and R are the detector outputs in millivolts.

The calibration model was tested by using the linear regression model in eq 1 to predict the concentrations of the remaining 19 samples. Figure 10 (square points) shows a plot of the predicted
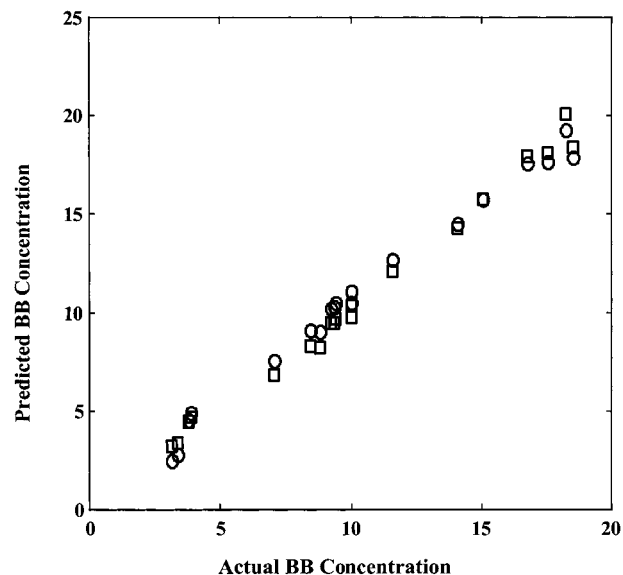

Figure 10. Predicted BB concentration vs actual BB concentration from detector difference measurements with optimum relative gain factor. Squares: linear model, SEP = 0.69 μM. Circles: third-order polynomial model, SEP = 0.60 μM.

BB concentrations versus the actual BB concentrations using this model. The SEP was determined to be 0.69 μM. On the basis of the appearance of nonlinearity in the calibration data, different nonlinear models were constructed from polynomial fits of increasing order. These nonlinear models were developed by assuming a polynomial correlation between $(T - KR)$ and concentration instead of the linear relation given in eq 8. Thus, the first 20 samples were used to obtain each of the possible models, and predictions based on these models were made for the remaining 19 samples. We observed that a third-order polynomial model provided the best improvement to the SEP (=0.6 μM). The improvement obtained by using these nonlinear models was relatively minor.

Discussion of Results. A number of factors exist to explain the disparity between the estimated linear SEP (0.69 μM) for MOC in this example and the expected SEP of 0.31 μM. First, we were

unable to calibrate the detectors because of instrumental limitations. Instead, data from the manufacturer's specifications were relied upon in determining detector spectral response. This information is of a general nature and better results are expected when all the individual optoelectronic components used in assembling the MOC measurement system are fully calibrated.

Second, fabrication errors resulting in the mismatch between the measured MOE spectrum and the theoretical spectrum can play an important role in the final results. An accurate reproduction of the MOE coating layers as specified by the design is necessary to achieve a value of the SEP that is comparable with that predicted for the design. The current process control system for the fabrication of MOEs does not provide the most effective means of monitoring the deposition process to produce layers with accurate thicknesses. Fortunately, many of the shortcomings of our current process control system can be rectified. These improvements will be the subject of future reports.

Third, normalization of the data was not performed. The acquisition of the test data in our laboratory was performed over the course of two 2-h sessions, so slight drift in the detectors probably contributes to our error. Normalization is an aspect of multivariate optical computation that will be the subject of a future report. A brief description of normalization and its hypothetical use in multivariate optical computing is given in ref 5. In brief, eqs 1 and 2 provide that the difference between transmitted and reflected rays in the Figure 1 instrument is related to the magnitude of a spectral vector (the regression vector) in the sample spectrum. The summation of the two responses, however, is directly proportional to the total magnitude of the spectrum. Corrections to the calibration data can be made so that they are suitable for measurement by calculating the ratio of the difference between T and R to the summation of T and R. This forms an implicit "normalization" of the spectrum during the prediction step and can be used to correct for prediction errors associated with power fluctuations and detector drifts.

Fourth, the lamp whose calibration we show in Figure 4C burned out early in our testing. Although a new lamp of the same type was installed and operated at the same voltage, there is no guarantee that the color temperature of the new lamp matched that of the old. This is an interesting problem that is common to many spectrometry systems using lamps and one that is ultimately addressable with MOC technology: a spectral vector for color temperature can be produced that will enable lamps to be controlled for color temperature. This problem is one that we are currently beginning to address and will also be the subject of a future report.

CONCLUSION

The concept of multivariate optical computing has been demonstrated with the successful design and testing of an MOE for the analysis of a binary dye mixture. The results obtained compare quite favorably with conventional PCR regression despite the nonidealities in sample measurement using the current prototype instrument, as well as those stemming from MOE manufacture. Measurements will be extended to the determination of chemical species in more complex systems with a greater number of interfering agents.

There exist several areas of theory that still need to be explored in order to gain a better understanding of MOC. For example, no theory has been developed covering the susceptibility of this technology to manufacturing errors. Also, the application of chemometrics to radiometric data has not been fully developed, so that there is currently no way to quantitatively predict the errors accumulated from nonlinearities in radiometry. All these areas are subjects of further study.

In general, we think it is important to keep in mind the following truth about multivariate optical computing: It is not a panacea. It is subject to all the same problems to which conventional multivariate spectroscopy is prone. In the case of weak signals or noisy detectors, it can hypothetically produce better SEPs than conventional spectroscopy; but it is no less sensitive to model or reference errors than conventional measurement techniques. Instead, MOC trades one set of problems for another. At the cost of a complex design and manufacturing process and the loss of some experimental flexibility, one gains a far simpler instrument with dramatically lower cost and maintenance. In our laboratory, for example, we estimate that the cost of producing the 26-layer MOE used here is much less than $100 per element when 50 or more are made. In some instances, multivariate optical computation is a tool that could make complex spectroscopic measurements accessible to a mass market.